

Supplementary Material for

**Parameter Sensitivity and Uncertainty Analysis of China's Terrestrial Carbon-Water  
Cycle Using a Dynamic Global Vegetation Model**

Fulai Feng <sup>a</sup>, Jianwu Yan <sup>a\*</sup>, Wei Liang <sup>a</sup>, Xiaohong Liu <sup>a</sup>, Bo Liu <sup>a</sup>, Xiaoru Liang <sup>a</sup>,  
Jia Wei <sup>a</sup>, Yangcan Bao <sup>a</sup>

<sup>a</sup> School of Geography and Tourism, Shaanxi Normal University, Xi'an, 710119,  
China

## Text S1. Detailed Methodology for Study Site Selection

### S1.1 Land Cover Data Preprocessing and Dominant Vegetation Type Determination

The land cover data source adopted in this study is the NASA MODIS MCD12Q1 product (2001-2023) (Friedl & Sulla-Menashe, 2022), which provides global land cover information for 17 IGBP (International Geosphere-Biosphere Programme) categories at a spatial resolution of  $0.05^{\circ}$ . To match the typical application scale of the LPJ-GUESS model, the original data were first resampled to a  $0.1^{\circ}$  resolution. During the resampling process, a spatial mapping relationship was established between the target  $0.1^{\circ}$  grid cells and the original four  $0.05^{\circ}$  sub-pixels, and the pixel proportion of each IGBP category within each  $0.1^{\circ}$  grid cell was calculated.

Subsequently, for each  $0.1^{\circ}$  grid cell, the multi-year average proportion of the 17 land cover types from 2001 to 2023 was computed. A clear threshold was set for determining the dominant vegetation type: only when the multi-year average proportion of the land cover type with the highest proportion within a grid cell exceeded 30%, and the difference between this proportion and that of the second-highest proportion type was greater than 10%, was the type with the highest proportion identified as the dominant vegetation type for that grid cell. Through this series of processing steps, a spatio-temporal vegetation distribution dataset was ultimately generated. This dataset, containing the latitude and longitude coordinates of each  $0.1^{\circ}$  grid, the identified dominant vegetation type number during the study period, and detailed proportion information for each type, served as the basis for site selection.

### S1.2 Detailed Sample Site Screening Steps

The screening of sample sites strictly followed these three core principles and operational steps:

**Nature Reserve Restriction:** Using GIS spatial overlay analysis, the vector boundaries of China's national nature reserves were intersected with the aforementioned  $0.1^{\circ}$  vegetation distribution dataset. Only grid points falling entirely within the boundaries of nature reserves were extracted as the initial candidate pool. This aimed to minimize significant disturbances from recent human activities on the natural state of vegetation.

**Natural Vegetation Type Screening:** From the initial candidate pool, non-natural or non-primary focus vegetation cover types in the IGBP classification, such as artificial surfaces (e.g., urban areas, croplands mixed with natural vegetation), and pure bare lands, were further excluded. The focus was on retaining grid points representing typical regional natural ecosystems, including various types of forests, grasslands, shrublands, savannas, and wetlands.

**Temporal Stability Verification of Vegetation Type:** To ensure the representativeness and stability of the ecological attributes of the selected sites during the study period, a consistency check of vegetation type was performed for each candidate site that passed the above screening. This was done for the entire observation period from 2001 to 2023. The specific method involved tallying the IGBP vegetation type identified for the site each year over the 23-year period. The vegetation type with the highest frequency of occurrence was then determined as the final, representative Plant Functional Type (PFT) for that site for subsequent analysis. This step effectively ensured the long-term stability of the core ecological attributes of the sample sites.

### **S1.3 Detailed Spatial Equilibrium Sampling Method**

After obtaining representative and stable candidate natural vegetation sites through the rigorous screening described above, a two-stage sampling strategy was designed and implemented. This was to ensure that the finally selected sample sites could comprehensively cover China's diverse natural vegetation types and be as geographically balanced as possible, thereby reducing potential biases in the analysis results due to spatial autocorrelation. The strategy is as follows:

**Category Assurance Sampling (First Stage):** Initially, all eligible candidate natural vegetation sites were grouped according to their represented IGBP land cover classification system. When selecting sites, it was mandatory that each major natural vegetation type (e.g., evergreen needleleaf forest, deciduous broadleaf forest, grassland, and other distinct IGBP categories) included at least one selected sample site. This measure aimed to ensure, from a typological perspective, that the study adequately considered and comprehensively covered China's vegetation diversity.

**Spatial Equilibrium Optimization (Second Stage):** When the planned total number of sample sites (set to 13 in this study) exceeded the total number of vegetation types that could be covered by the first stage, a spatial equilibrium optimization sampling procedure was initiated to select the remaining sites. The core idea of this procedure was to prioritize, through iterative selection, candidate sites that could maximize their geographical distance from the existing set of selected sample sites. Specifically, for each unselected candidate site, the shortest Euclidean distance to all already selected sample sites was calculated. The candidate site with the largest shortest Euclidean distance was then added to the sample set. This process was repeated until the predetermined total number of samples was reached. This iterative selection method aimed to effectively reduce the spatial clustering effect and autocorrelation among the finally selected sample sites, promoting a more uniform and dispersed distribution of sites on a national geographical scale. This, in turn, allows for a more scientific and unbiased representation of the macroscopic ecological environment characteristics of different regions in China.

## Text S2: Detailed Sensitivity Analysis by Parameter Type

### S2.1 Sensitivity Analysis of Physiological Process Parameters

To further clarify the role of different parameter types, this section first focuses on the sensitivity of the 19 physiological process parameters (Fig. S2). When considering only physiological parameters, *ALPHA\_C3* (intrinsic quantum efficiency of CO<sub>2</sub> uptake for C3 plants) exhibited the most prominent sensitivity, showing the highest sensitivity to almost all nine output variables. Its standardized sensitivity index was close to or reached 1.0 across all three methods, indicating that the quantum efficiency of photosynthesis is the core physiological parameter regulating the ecosystem carbon-water processes in the model.

*THETA* (photosynthesis co-limitation shape parameter) was the second most important physiological parameter, showing moderate to high sensitivity to variables such as GPP, Soil Carbon Flux, and LAI. The *GM* (maximum canopy conductance equivalent) parameter, which directly regulates water transpiration, showed extremely high sensitivity to Actual Evapotranspiration (AET) and a significant impact on Net Ecosystem Exchange (NEE). The analysis also revealed that NEE exhibited a relatively broad sensitive response to multiple physiological parameters, including *K\_BEER* (light extinction coefficient), *ALPHAM* (empirical parameter for evapotranspiration), and *FRADPAR*. In contrast, physiological parameters related to fire occurrence (*MINFUEL*) and specific litter decomposition processes (*TAU\_LITTER*, *ATMFRAC*) generally showed low sensitivity to the various output variables in the current analysis.

### S2.2 Sensitivity Analysis of PFT Constitutive Parameters

Next, this section analyzes the sensitivity of the 20 parameters related to Plant Functional Type (PFT) constitution (Fig. S3). The results clearly indicate that *common\_reprfrac* (proportion of NPP allocated to reproduction) is the most critical PFT parameter. Its sensitivity to all nine output variables was significantly higher than other PFT parameters across all three analysis methods. This highlights the decisive regulatory role of vegetation reproduction and biomass allocation strategies on ecosystem carbon-water dynamics.

Among other PFT parameters, *tree\_turnover\_root* (fine root turnover rate) showed particularly high sensitivity to Litter Carbon stock (Litter C) and Total Carbon stock (Total C), especially under the Morris method where its sensitivity index approached 0.88. *shade\_tolerant\_est\_max* (maximum seedling establishment rate for shade-tolerant tree species) had a relatively significant impact on NEE, as well as on Vegetation and Litter Carbon stocks. Furthermore, some PFT parameters related to tree structure (e.g., *tree\_k\_allom2*) and the relationship between leaf and sapwood area (e.g., *broadleaved\_k\_latosa*) also showed moderate

sensitivity to variables such as LAI and Vegetation Carbon. The sensitivity patterns of different output variables to PFT parameters also varied. For instance, GPP was strongly influenced by a few PFT parameters (mainly *common\_reprfrac*), while various carbon stock variables were sensitive to a broader range of PFT parameters (especially those related to carbon allocation and turnover).

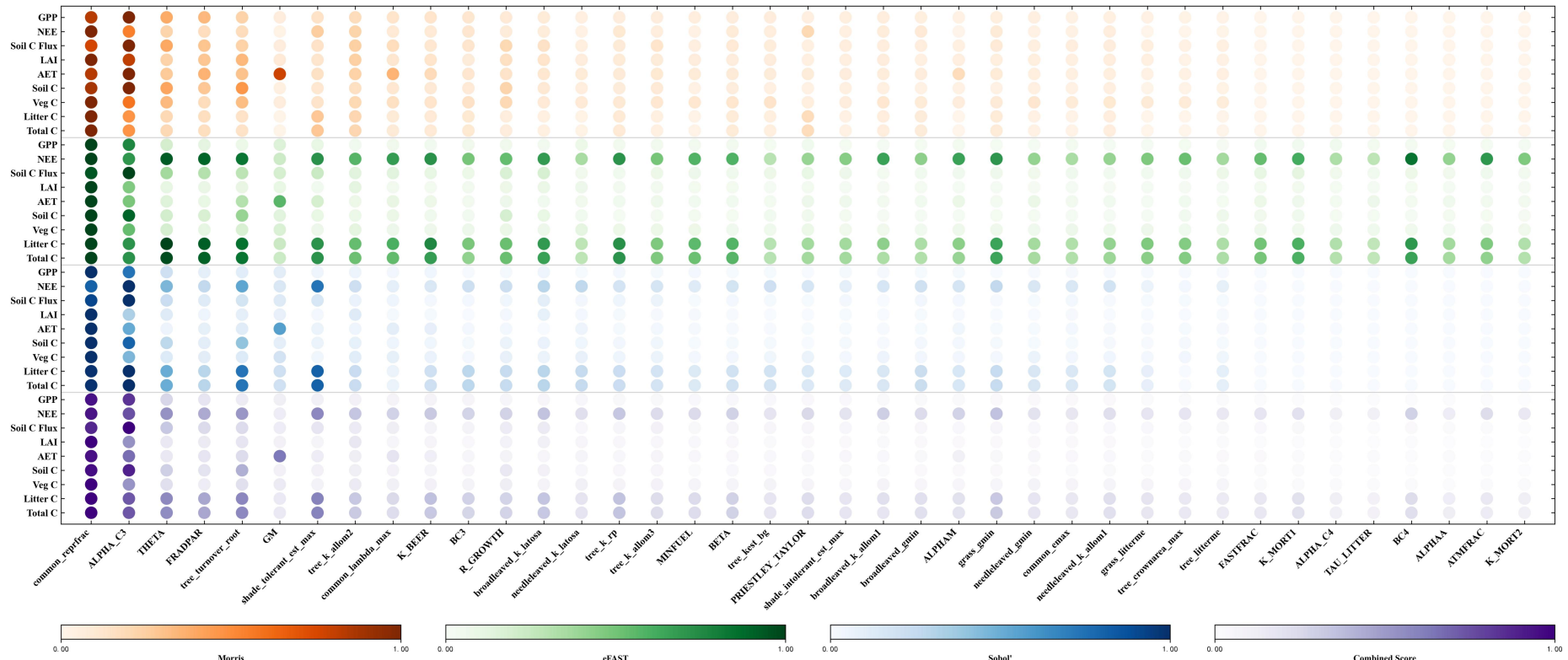


**Fig. S1: Sensitivity Results of All Parameters for Nine Different Target Variables Using Different Methods**

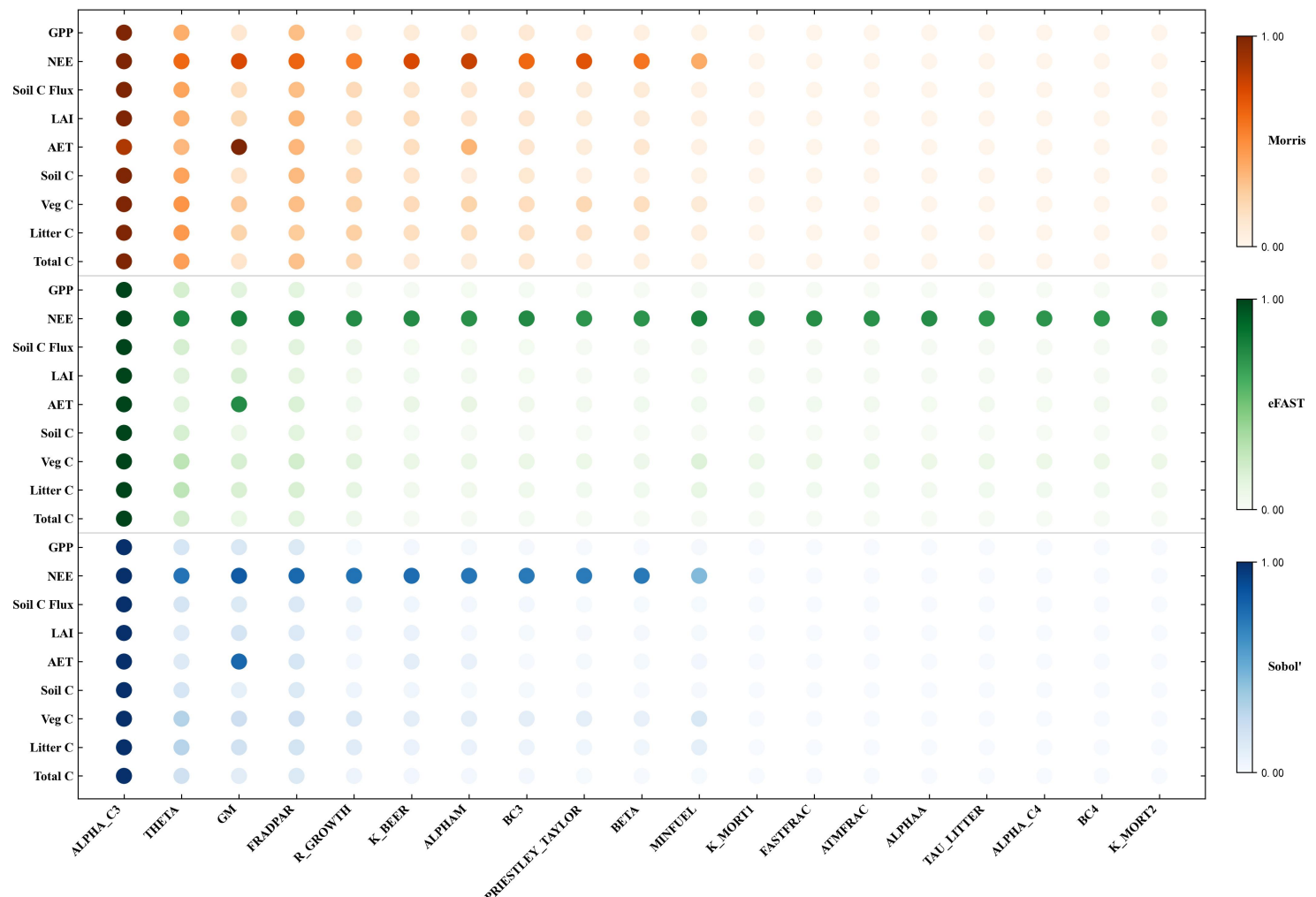


**Fig. S2: Physiological Process Parameters for All Target Variables Across Different Methods**

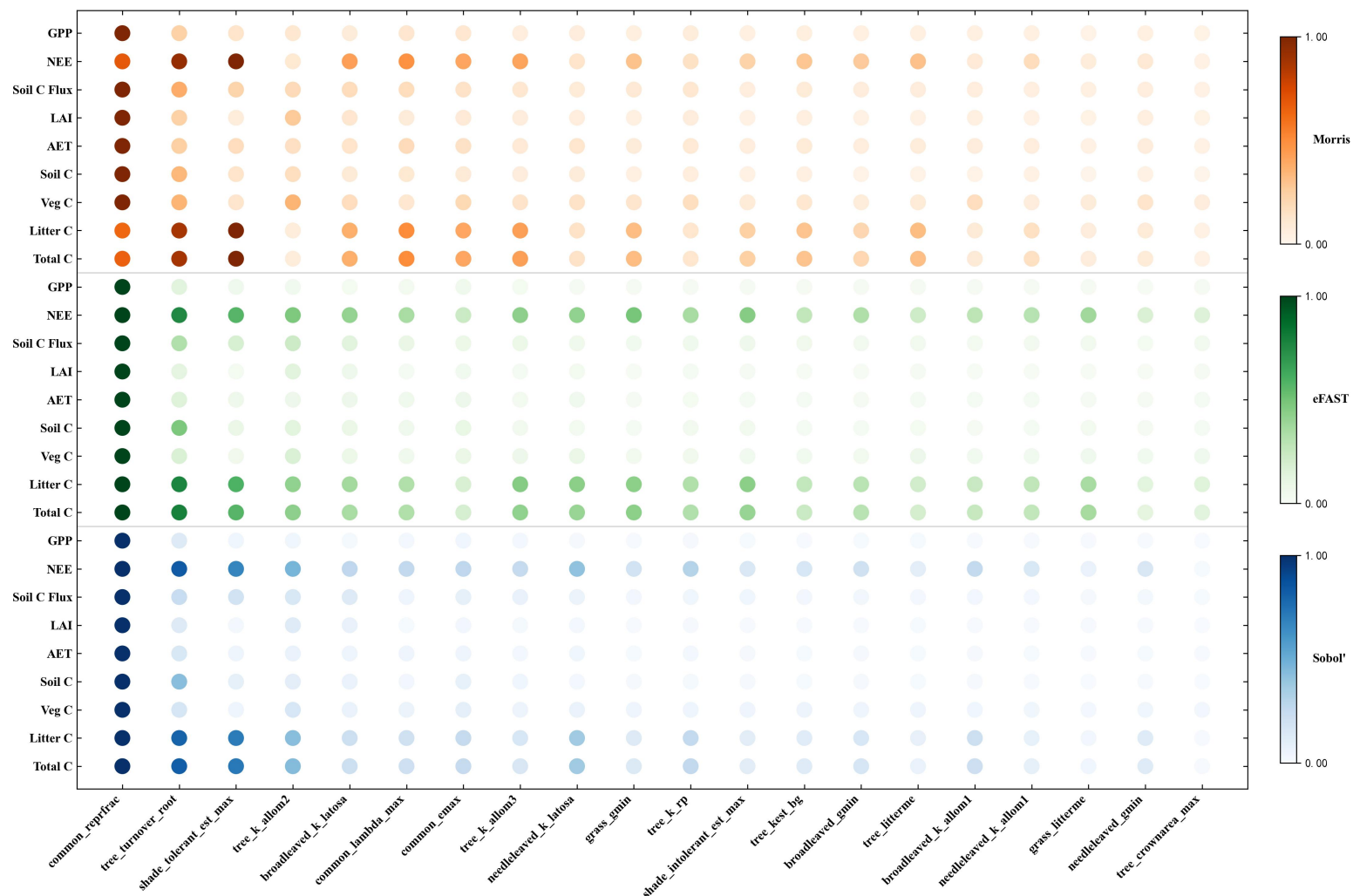


**Fig. S3: PFT Composition Parameters for All Target Variables Across Different Methods**

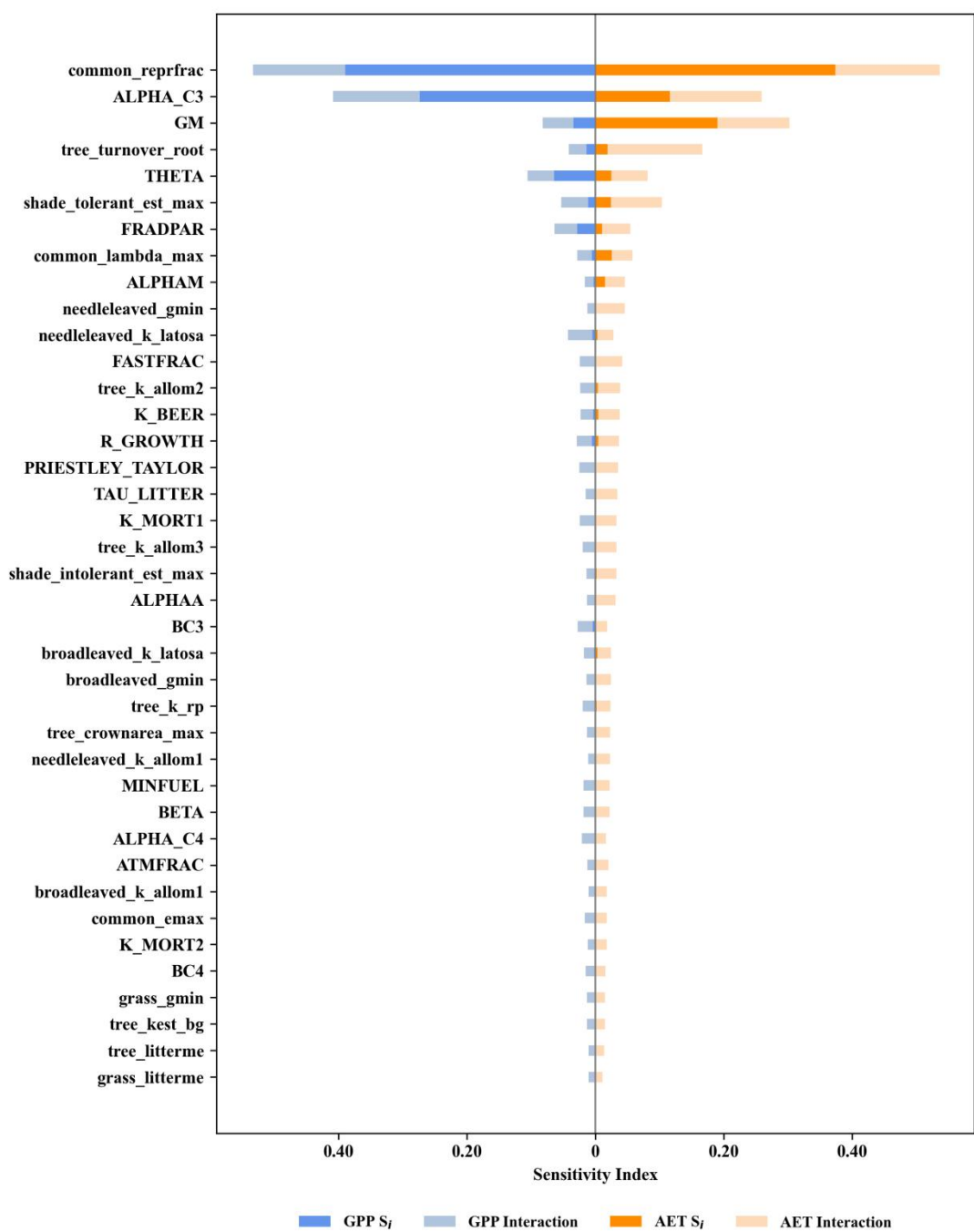


**Fig. S4. Decomposition of parameter sensitivity for GPP and AET into main effects (S<sub>i</sub>) and interaction effects based on the eFAST method**

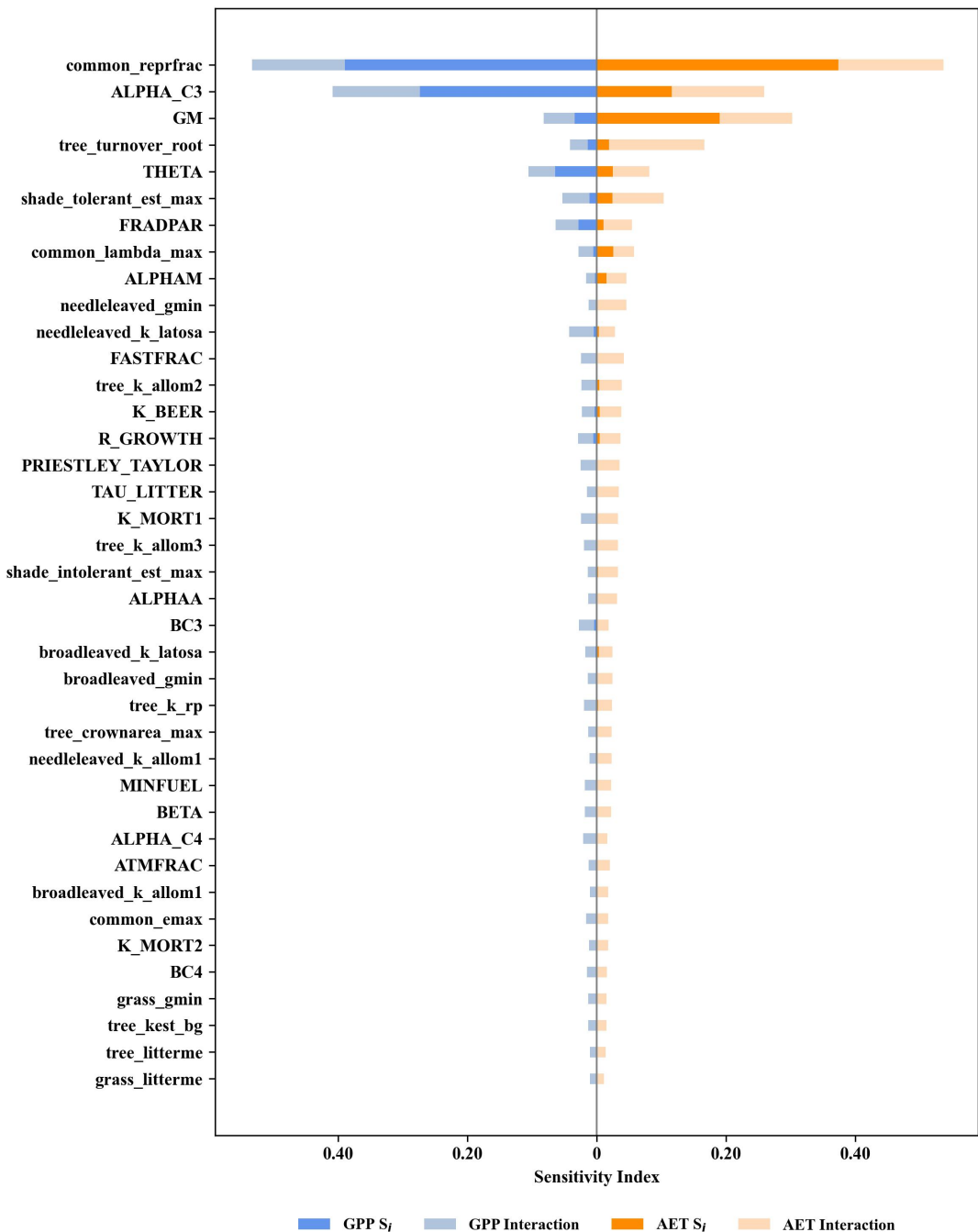


**Fig. S5. Decomposition of parameter sensitivity for GPP and AET into main effects ( $S_i$ ) and interaction effects based on the Sobol' method.**

**Table S1 IGBP types at each site and their corresponding dominant PFT types in LPJ-GUESS**

<b>ID</b>	<b>Lon</b>	<b>Lat</b>	<b>IGBP</b>	<b>IGBP full name</b>	<b>LPJ-GUESS PFT</b>
1	85.4	41.3	BSV	barren or sparsely vegetated	C3G
2	88.3	31.8	GSL	grasslands	C3G
3	116.8	44.1	GSL	grasslands	C3G
4	112.9	28.8	SAV	savannas	TeBS + C3G
5	105.3	37.8	OSH	open shrublands	IBS + C3G
6	109.1	31.9	DBF	deciduous broadleaf forest	TeBS
7	104.3	32.9	MF	mixed forests	TeBS + TeNE
8	117.8	27.8	EBF	evergreen broadleaf forest	TeBE
9	103.3	34.5	WSV	woody savannas	TeBS + C3G
10	98.7	25.5	ENF	evergreen needleleaf forest	TeNE
11	118.8	30.8	CNV	cropland/natural vegetation mosaic	TeBS + C3G
12	109.1	21.6	PWL	permanent wetlands	TrBE + C3G
13	120.6	51.8	DNF	deciduous needleleaf forest	BNS